JOURNAL OF BACTERIOLOGY, Sept. 1993, p. 5953–5961
0021-9193/93/185953-09$02.00/0

Vol. 175, No. 18

A Ring-Shaped Structure with a Crown Formed by Streptolysin O on the Erythrocyte Membrane

KACHIKO SEKIYA,[1]* RYOHEI SATOH,[2] HIROFUMI DANBARA,[1] AND YUTAKA FUTAESAKU[3]

Department of Microbiology, School of Pharmaceutical Sciences, Kitasato University, Minato-ku, Tokyo, 108 Japan,[1] and Department of Physiology, School of Medicine,[2] and Laboratory of Ultrastructure Research, School of Hygienic Sciences,[3] Kitasato University, Sagamihara, Kanagawa, 228 Japan

Received 12 March 1993/Accepted 21 July 1993

Streptolysin O (SLO) is a membrane-damaging toxin produced by most strains of group A beta-hemolytic streptococci. We performed ultrastructural analysis of SLO-derived lesions on erythrocyte membranes by examining electron micrographs of negatively stained preparations. SLO formed numerous arc- and ring-shaped structures with or without holes on membranes. Rings formed on intact cell membranes had an inner diameter of ca. 24 nm and had distinct borders of ca. 4.9 nm in width, but the diameter of rings varied from 24 to 30 nm on membranes of erythrocyte ghosts. Image analysis of electron micrographs demonstrated that each ring was composed of an inner and an outer layer. Each layer contained an array of 22 to 24 SLO molecules. On the top of the ring, we found a characteristic crown that projected from the cell membrane. The crown was separated by an electron-dense layer from the basal part of the ring that was embedded in the lipid bilayer of the erythrocyte membrane. Heights of the three parts, namely, the crown (head), the space (neck), and the basal portion (base), were ca. 3.2, 1.6, and 5.0 nm, respectively, and we postulated that these parts are the constituents of a single SLO molecule. The volumes of SLO molecules in the inner and outer layers were calculated to be 77 and 88 nm^3. On the basis of a model of the structure of SLO, we propose some new details of the mechanisms of hemolysis by SLO toxin.

Streptolysin O (SLO) is a membrane-damaging protein toxin. It is known as a thiol-activated or oxygen-sensitive toxin and is produced in the extracellular medium by most strains of group A beta-hemolytic streptococci (1–3, 6, 17, 21).

It has been shown by electron microscopy that SLO forms arc- or ring-shaped structures (arcs or rings) on erythrocyte membranes as do other thiol-activated toxins after binding to cholesterol molecules (7, 9, 12, 13).

Two hemolytic forms of SLO molecules have been reported: an acidic type with a molecular weight of 69,000 ± 3,000 and a pI of 6.0 to 6.4 and a neutral and degraded type of 57,000 ± 5,000 in molecular weight with a pI of 7.0 to 7.5 (4).

The calculated volume of the ring indicates that one ring is composed of between 20 and 100 monomers of the toxin molecule (4, 6). Results of hemolytic titrations indicate that 70 to 125 monomers of SLO are required for formation of a single functional lesion on an erythrocyte (4). However, the mechanism of hemolysis after formation of these rings is not known. There are also no definitive reports on the ultrastructure of the rings.

In this report, we describe the presence of a crown on the top of an SLO ring and the arrangement of the discrete SLO molecules in the ring. We also propose a model for the ring that involves discrete molecules of SLO.

MATERIALS AND METHODS

Preparation of SLO. The toxin was kindly provided by Noboru Nakagawa (The Kitasato Institute, Tokyo, Japan), and it was prepared by a modified version of the methods of Suzuki et al. (18) and Duncan and Schlegel (9) as follows. A total of 40 liters of Todd-Hewitt broth (Difco Laboratories, Detroit, Mich.) was inoculated with 1,000 ml of an overnight culture of group A streptococci (Richard strain) with the pH maintained at 7.0. After incubation for 17 h, the culture was placed overnight in a cold room and then centrifuged. The supernatant was saturated with ammonium sulfate. After centrifugation, the pellet was dissolved in phosphate-buffered saline (pH 6.0), dialyzed, and stored at −80°C. The hemolytic activity of SLO was expressed as the 50% hemolytic dose per milliliter (18), and it was 7×10^3 50% hemolytic doses per milliliter.

Preparation of erythrocyte membranes. Fresh rabbit blood was purchased from Nippon Bio-Test Laboratories Inc. (Tokyo, Japan). The blood cells were washed in physiological salt solution (Ohtsuka Pharmaceutical Co., Tokyo, Japan) two or three times and were finally suspended at a concentration of 50% (vol/vol). A total of 40 μl of the 50% suspension of erythrocytes was mixed in a test tube with 20 μl of SLO that had been activated by treatment with 20 to 25 mM cysteine or 50 mM 2-mercaptoethanol. The mixture was incubated at 37°C for 10 min. Then, 20 μl of the suspension of lysed erythrocytes was dropped onto the surface of distilled water (ODW; Ohtsuka Pharmaceutical Co.) in the hollow of a plastic bottle cap by a modified version of the method of Nicolson and Singer (14). After 20 to 30 min, the membrane fragments floated and spread out over the air-water interface. The floating fragments were mounted on supporting films of Butval-98 or carbon on grids by placing the grids gently on the surface of the water and leaving them there for 1 min.

Preparation of ghost membranes. A 3-ml sample of the 50% suspension of erythrocytes that had been washed in physiological salt solution was added to 7 ml of ODW, and the mixture was centrifuged at 27,000 × *g* for 20 min. The supernatant was discarded. The pellet was suspended in

* Corresponding author.

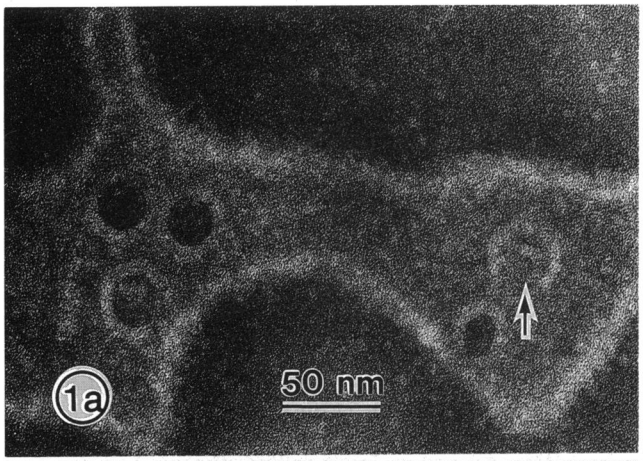

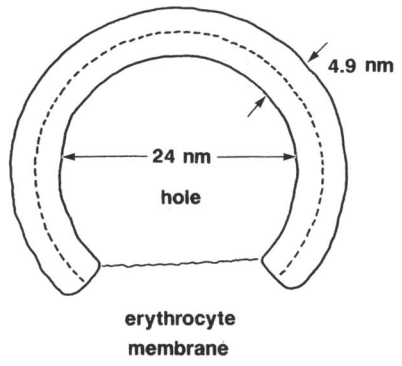

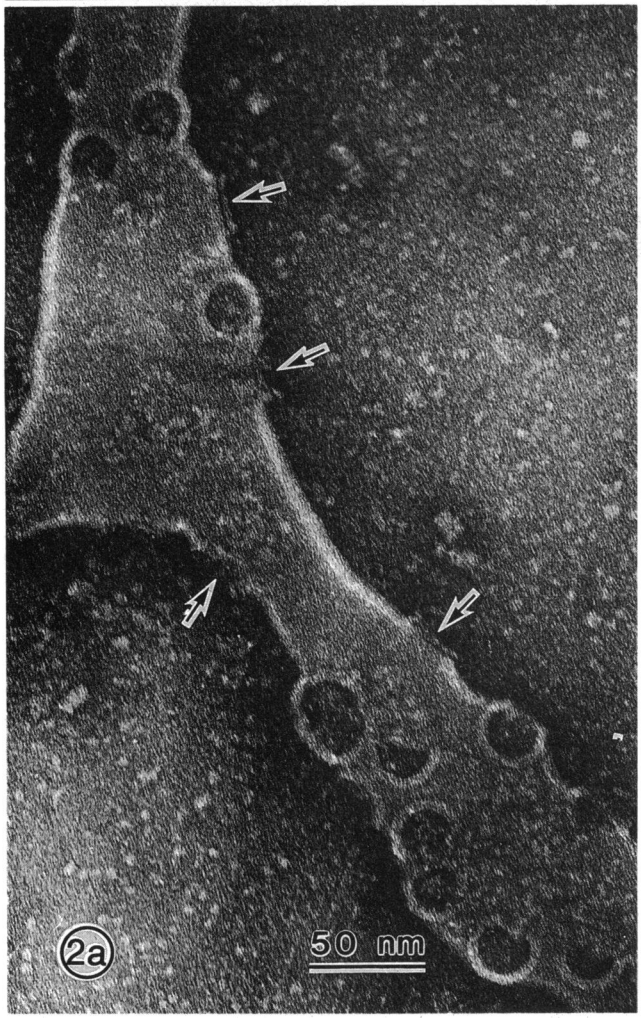

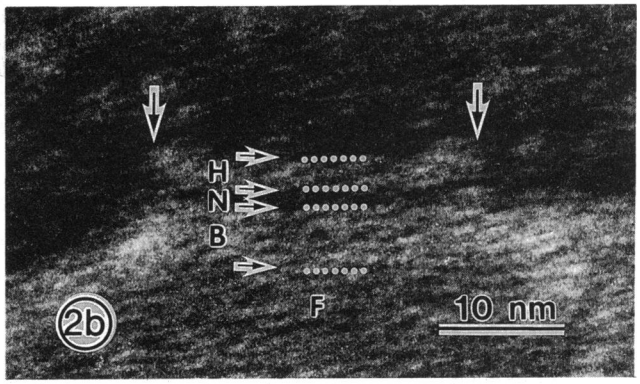

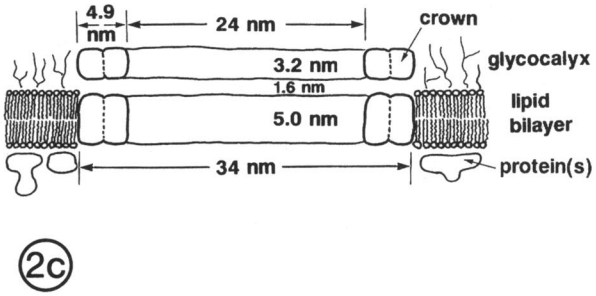

FIG. 1. (a) Electron micrograph of a rabbit erythrocyte that had been lysed by treatment with SLO. The specimen was fixed with glutaraldehyde before negative staining with PTA. Note both arcs and rings with holes and an arc without a hole (arrow). (b) Schematic drawing of an incomplete ring on an erythrocyte membrane.

FIG. 2. (a) Electron micrograph of a rabbit erythrocyte that had been lysed by treatment with SLO. In the case of rings on the folded edge of the erythrocyte membrane, crowns (arrows) on the rings can be observed. The folded edges of the membrane without an SLO ring are electron sparse, while those with an SLO ring are electron dense. (b) A high-power electron micrograph of the same crown as in panel a. A crown is shown between two downward arrows. The head (H), neck (N), and base (B) parts were measured between the bars indicated by transverse arrows. The electron density of the basal part was weaker than that of the flat area (F) of the erythrocyte membrane. (c) Schematic drawing of a crown on an erythrocyte membrane.

physiological salt solution and washed once or twice by centrifugation. The suspension of erythrocyte ghosts was then dropped onto ODW as described above, and the floating ghost membranes were mounted on supporting films on grids. Then, the membranes were treated with SLO by floating the grids on 20-μl droplets of SLO at room temperature or at 37°C for various intervals of time.

Electron microscopy. The membrane fragments were fixed with 2.5% glutaraldehyde for 1 min at room temperature, washed with ODW, and then negatively stained with 2% phosphotungstic acid (PTA), pH 7.4, that contained 0.2% (wt/vol) sucrose. Specimens were observed under a transmission electron microscope (JEOL 2000 EX or Hitachi H-500). The diameters and borders of SLO were calculated from 50 rings on photocopies of electron micrographs at a final magnification of 0.9×10^6 to 1.0×10^6.

Image analysis. Densitometric and three-dimensional analyses of electron micrographs at a magnification of 0.9×10^6 to 1.0×10^6 were performed with a computerized image processing system composed of an image scanner (GT-4000; EPSON, Tokyo, Japan) and an Apple Macintosh II-based software package (IMAGE) that had been developed by W. Rasband at the National Institute of Mental Health, Bethesda, Md. Any area of the electron micrographs of SLO could be scanned with the image scanner, and the images were digitized with 8-bit intensity resolution (256 levels of gray from 0 [black] to 255 [white]) and stored in the computer for later image processing and analysis. Before image processing, a common smoothing filter was applied to the original electron micrographs.

RESULTS

Negative staining of erythrocyte membranes that had been damaged by SLO revealed numerous arcs and rings with distinct borders of 4.9 ± 0.1 nm in width, an internal diameter of ca. 24 nm, and an outer diameter of ca. 34 nm (Fig. 1a and b). The lengths of arcs varied, but the radii were almost the same in every case. Most rings, and even the semicircular arcs, had an electron-dense center after negative staining with PTA. Thus, it appeared that a hole was present in the inside of each ring or arc (Fig. 1a and 2a), but a few arcs had no holes (Fig. 1a).

A crown-shaped structure (crown) was found on top of the rings observed from the side, in cases in which rings were on the edges of membranes (Fig. 2a and b). Each ring was composed of three layers, with an electron-sparse top, a dark middle layer, and a basal part that was embedded in the erythrocyte membrane (Fig. 2b). The heights of each layer were as follows: ca. 3.2, 1.6, and 5.0 nm, respectively (Fig. 2c).

In the experiment with ghost membranes, the holes in the rings varied from 20 to 40 nm in diameter (Fig. 3). The rings were observed not only on ghost membranes, but also on supporting films without any biological membranes in the same field (Fig. 4). When the rings on the supporting films were photographed, their profiles, which were emphasized by phase contrast, indicated that an inner and an outer layer together formed one ring and that each layer had 22 to 24 inner units (unit-I's) and the same number of outer units (unit-O's) (Fig. 5). When they were just in focus, the images of the rings (Fig. 6a) and densitometric (Fig. 6b and c) and three-dimensional image analyses (Fig. 6d and e) confirmed the double-layered structure of and the discrete arrays of electron-sparse units in each ring.

In the inner layer, the unit-I's were closely packed together with partial overlapping when viewed from the center of the ring. If the number of units in one layer was fixed at 22, the central angle subtended by a single unit was 16.4°. The tilting angle of each unit to a tangent of the inner circle was 16.4° on the intact cell membrane (Fig. 7).

In the outer layer, gaps were observed among the unit-O's, which were arranged in parallel with unit-I's and formed pairs with them. Therefore, the positions of units in the two layers alternated when viewed from the center of the ring (Fig. 7).

The rings on ghost membranes were analyzed by the same method and gave similar results (Fig. 8).

To estimate how many SLO molecules might occupy the space of one unit, volumes of unit-I and unit-O were calculated with the three dimensions of inner and outer diameters (Fig. 1a and b), as well as the heights of the crown and the basal part of each member of a ring (Fig. 2). When the number of units in one ring on an intact cell membrane was taken as 44 (Fig. 5), the calculated volume of a unit-I was 77 nm^3 and that of a unit-O was 88 nm^3 (Fig. 9).

DISCUSSION

SLO produced characteristic lesions of uniform size, which appeared as arcs and rings on erythrocyte membranes in electron micrographs after negative staining. The outer diameter of SLO rings on intact cell membranes was ca. 34 nm. The width of the distinct border was ca. 4.9 nm, and it

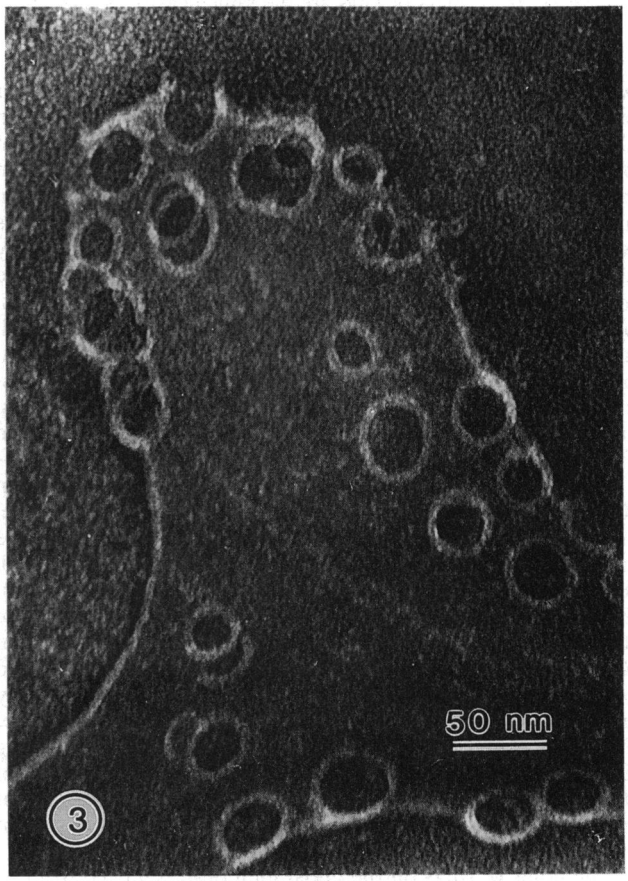

FIG. 3. Electron micrograph of rings formed by SLO on a ghost membrane. Note the variations in the sizes of the rings.

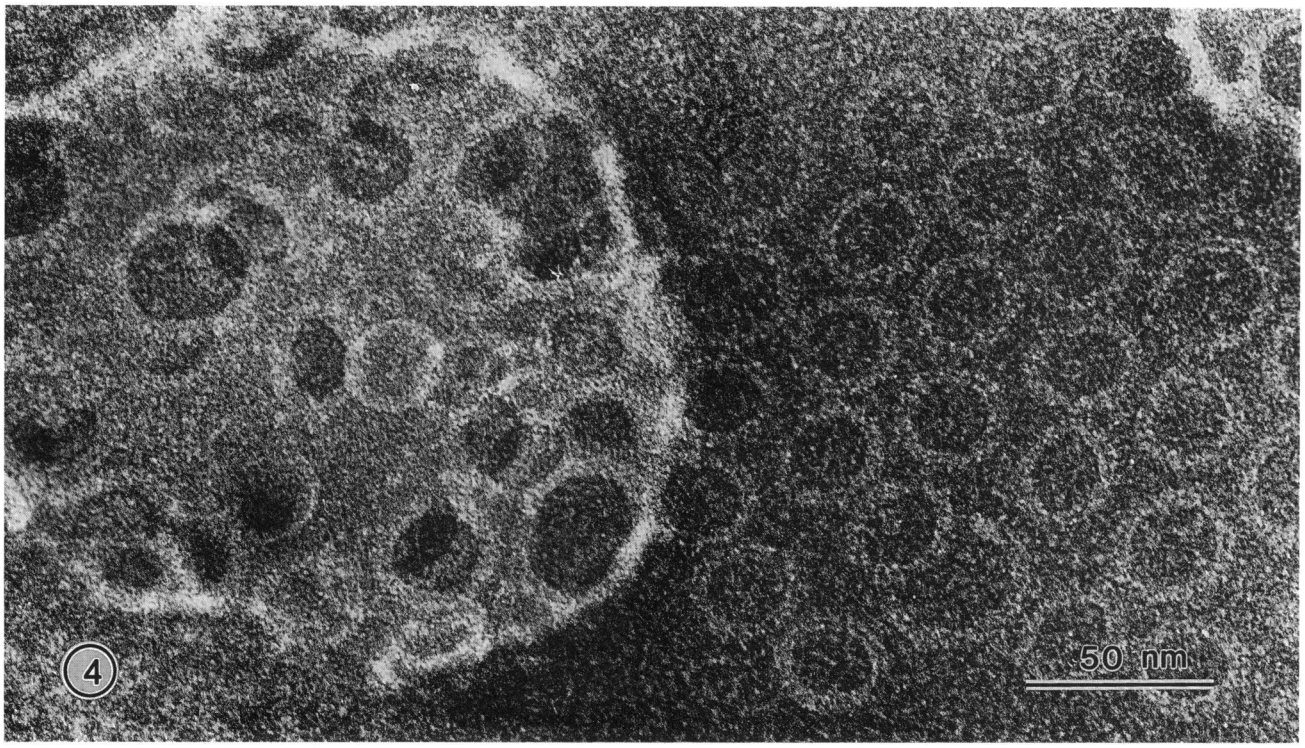

FIG. 4. Electron micrograph of rings formed on a membrane (left side) and on the supporting film without a membrane (right side). In the latter case, the centers of rings are the same density as the area outside the rings.

was narrower than the 7 to 7.5 nm reported from other studies (2, 7, 9) but similar to that of rings of perfringolysin O reported by Mitsui et al. (12, 13). The present results might be due to the fact that the specimens were supported on thin carbon films and photographed under minimum illumination at a high-power magnification of ×100,000. If the specimens were illuminated by a stronger beam of electrons, they suffered illumination damage and their fine structures were lost (data not shown). A wide border of ca. 7 nm was, however, observed on supporting films in the absence of cell membranes (Fig. 4 and 5), as reported for SLO-SH complexes by Niedermeyer (15). The unit-O's might be loosened, because there is no membrane around the rings. Indeed, the heights of unit-O are less than those of unit-I in Fig. 6d and e.

The dark hole in the center of a ring was 24 nm in diameter, as previously reported by Duncan and Schlegel (9). The holes were not observed on plasmatic fracture faces from fresh membranes (15). However, freeze fracture with fixation by glutaraldehyde revealed holes on both faces (7). The metal coating with heat evaporation might cause the dislocation of small molecules, such as lipids, since rings of SLO that penetrated both layers of membranes were found only on the exoplasmatic face after a fracture, while only traces of hollows remained on the plasmatic fracture face. The hole may cause a leak in the membrane by repelling lipids from the hydrophilic area on the concave surfaces of the ring. Once the ring has a hole in its center, the ring might be subject to forces from its convex side as a result of surface tension of the cell membranes.

The holes of rings on the ghost membranes varied from 20 to 40 nm in outer diameter. Such variations might result from the difference in surface tension between the two types of membrane. The surface tension on the ghost membrane might be weaker than that on the intact cell membrane.

A crown was observed on the top of SLO rings when the rings formed on the folded edges of the erythrocyte membrane were viewed from the side (Fig. 2a). A high-power electron micrograph (Fig. 2b) demonstrated that the structure of the SLO ring was characterized by a set of electron-sparse crown (head), electron-dense space (neck), and electron-sparse basal (base) parts. It should be noted that electron density is different between the basal part of the SLO ring and the flat area of the erythrocyte membrane; that is, the former is more sparse than the latter. This difference seemed to be explained by the flat area of erythrocyte membrane, but not the membrane struck by SLO molecules, being easily penetrated and filled with PTA, resulting in an electron-dense micrograph. This explanation is supported by the fact that the folded edges of the membrane are electron sparse (Fig. 2a). This might be caused by little or no PTA penetration of the folded edges with packed-lipid molecules. These results strongly suggested that the basal part of the SLO ring is embedded in the lipid bilayer of the erythrocyte membrane. The structure projecting from the erythrocyte membrane was similar to the cylindrical structure of the membrane attack complex that is seen on membranes after complement-mediated lysis, but the total height of the SLO ring was approximately 10 nm and was less than that of the ring formed by the C5b-9 complex (5, 19). The thickness of the erythrocyte membrane is considered to be approximately 10 nm, including the surface coat of glycocalyx, a lipid bilayer, and supporting proteins underneath the membrane from which proteins can be removed after treatment with both trypsin and chymotrypsin (7). Therefore, negative staining allows us to see only the lipid-bilayer part (5 to 6 nm)

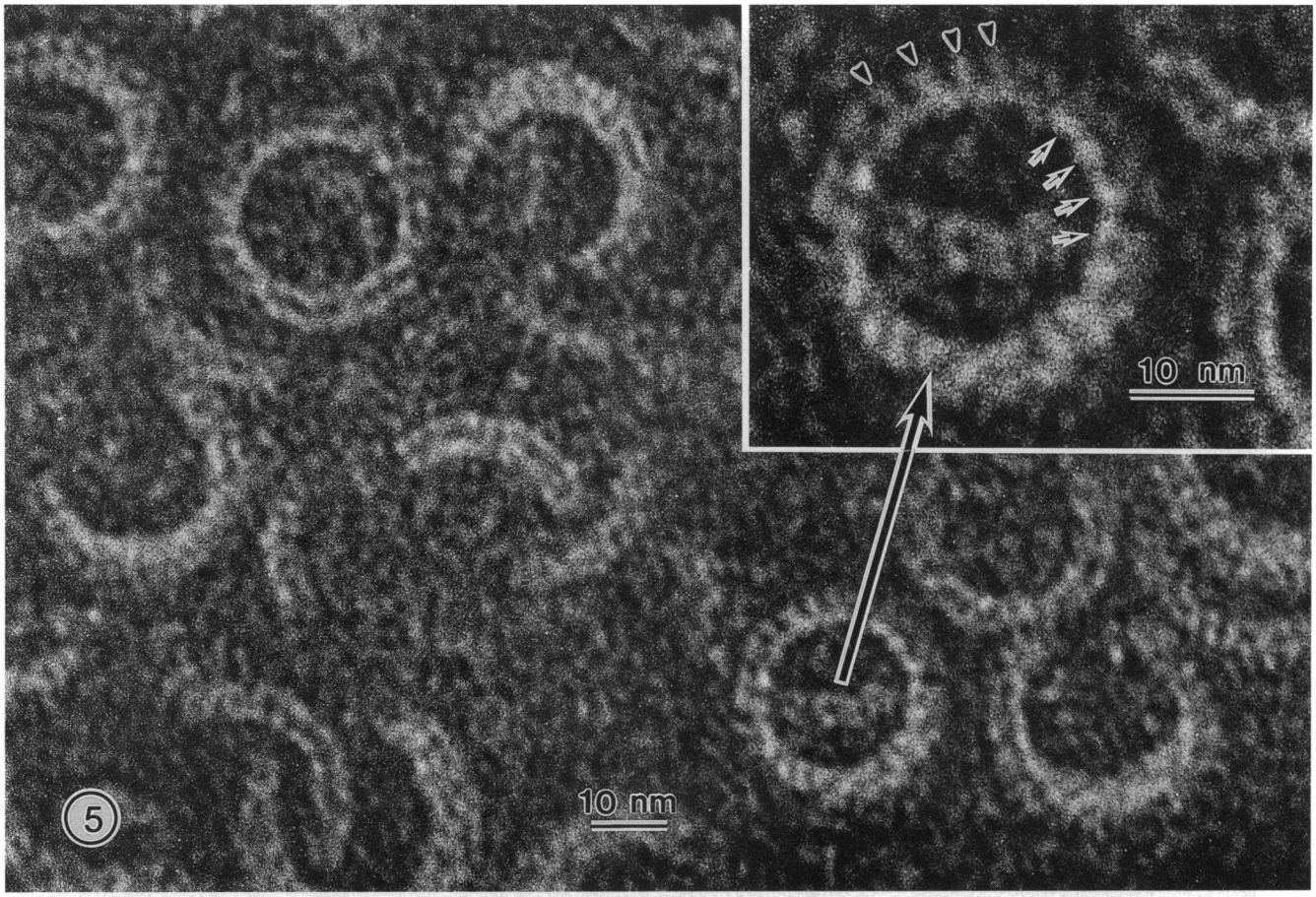

FIG. 5. Electron micrograph of rings on a supporting film photographed with underfocusing. Note that one ring is enlarged and shown in an inset; it is composed of inner (arrows) and outer (arrowheads) layers with 22 to 24 electron-sparse units per ring.

of the cell membrane, since PTA can penetrate the layer of glycocalyx.

The volumes of unit-I and unit-O were calculated (Fig. 9). The molecular weight of SLO has been reported to be about 69,000 in the case of a protein with a pI of 6.0 to 6.4 (acidic-type SLO) and 57,000 in the case of a protein with a pI of 7.0 to 7.5 (neutral-type SLO) by Bhakdi et al. (4). A molecular weight of 63,645 was calculated for a protein with 571 amino acid residues by Kehoe et al. (11), and values of 64,000 were proposed for the acidic and neutral types of SLO by Suzuki et al. (18). The molecular weight of microtubules has been reported to be 55,000 for monomers (8), and the calculated volume [$2 \times (5\ \text{nm}/2)^2 \times 8\ \text{nm}$] was 157 nm^3 for a dimer of α and β subunits from measurements made on electron micrographs after negative staining and optical diffraction (10). A similar calculation yields a volume of approximate 80 to 90 nm^3 for the basal and crown parts of SLO, respectively, and is just equal to the volume of one SLO molecule. Although both the density and hydration of the two proteins are ignored in such calculations, the values are still not far from the 90 nm^3 reported by Niedermeyer (15) and by Bhakdi et al. (7), which were calculated from a total volume of 6,000 nm^3 for a ring of 7.5 nm in width. Therefore, unit-I seems to correspond to one SLO molecule on the inner layer (SLO-I) and unit-O seems to correspond to one SLO molecule on the outer layer (SLO-O). There is, however, no indication whether SLO-O and SLO-I correspond to the acidic-type SLO and the neutral-type SLO, respectively.

When an SLO ring is present on a lipid bilayer, the outside of the ring must have a hydrophobic zone (7). In contrast to the outside, the inside of the ring where there is a hole must enclose a hydrophilic zone (7). It is hard for SLO to form a ring under conditions in which cholesterol or cell membranes are not present. Sufficient amounts of cholesterol stabilize SLO molecules and allow formation of rings in an aqueous environment without a lipid bilayer (9). Bhakdi et al. (7) have reported that the amount of cholesterol by weight in SLO-treated membrane samples was no more than 1 to 1.5%. It was concluded that the SLO rings extracted from erythrocyte membranes contain fewer than two cholesterol molecules (molecular weight, ca. 387) per SLO molecule (molecular weight, ca. 69,000). The SLO rings penetrated the phosphatidylcholine liposomes without additional cholesterol molecules (7). Therefore, cholesterol may be required on the hinges between the SLO molecules when they bind laterally to each other to form rings.

It has been suggested that sulfhydryl groups have a role in the formation of rings, but this suggestion depended on the SLO molecule having two Cys residues. However, analysis of the DNA sequence revealed that a single SLO molecule has only one Cys residue (11, 16, 20). At the present time, it seems unlikely that SLO molecules bind to their neighbors via —SH groups to form oligomers (16). It is possible,

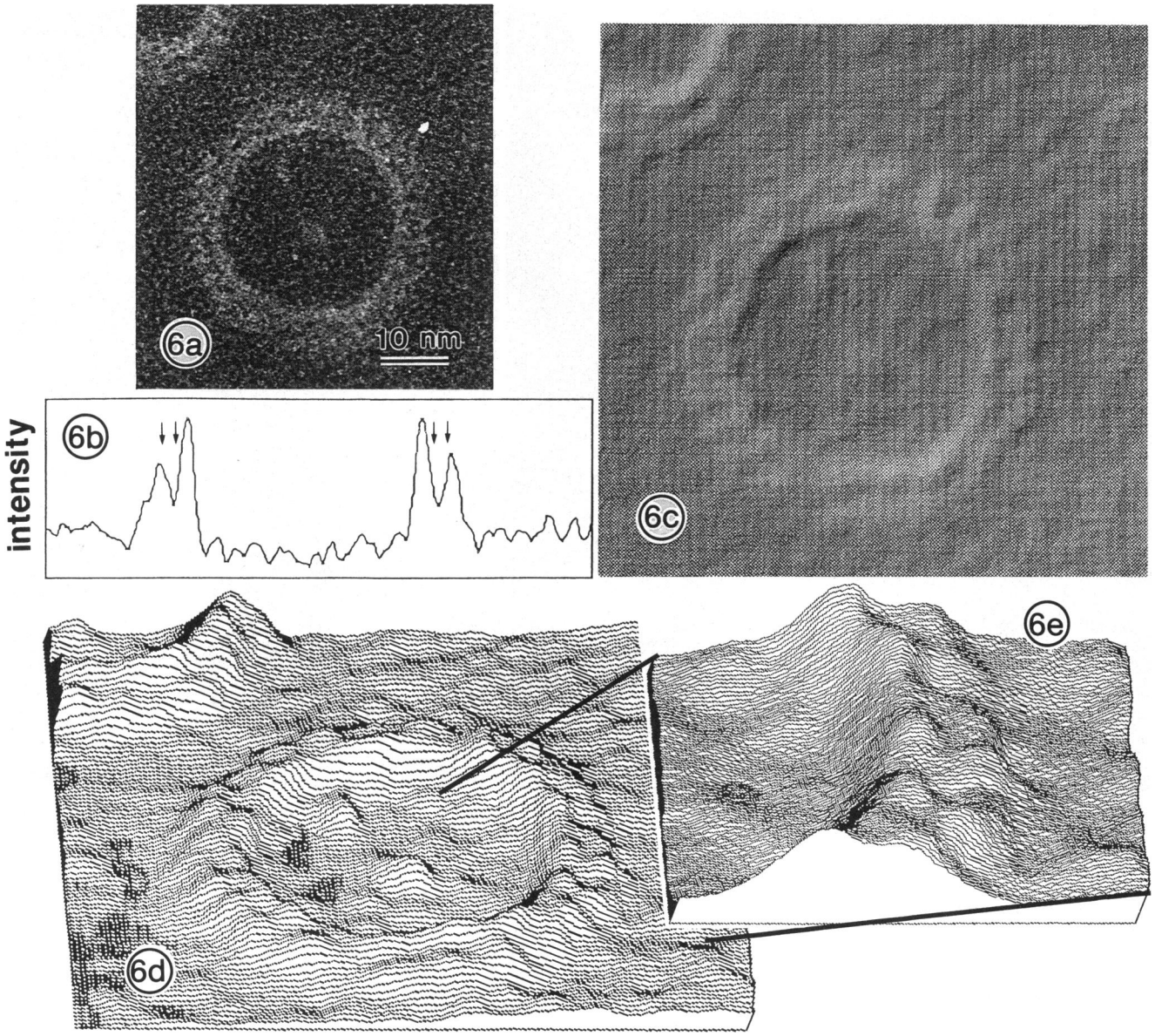

FIG. 6. (a) Electron micrograph of a ring on a supporting film photographed when it was just in focus. The figure was analyzed three-dimensionally with the image analyzer (b to e). (b) A densitogram across the center of the ring and both distinct borders of the ring shows two layers (double arrows). (c) Two-dimensional densitometry reveals the units in both layers. (d and e) Three-dimensional projection, enhanced to show the arrangement of units in both layers.

however, that SLO molecules form dimers that are stabilized in aqueous solution. An SLO dimer might be stabilized by the —SS— bond and solubilized in aqueous environments since it is well known that the presence of albumin is important for stabilizing the hemolytic activities of solutions of SLO (4). An —SS— bond within an SLO dimer could, however, mask the bilateral binding sites required for formation of a ring, or it could mask a hydrophobic site on the molecular surface that could penetrate an apolar domain of a lipid bilayer. Furthermore, since a certain amount of a thiol compound is necessary for ring formation, —SS— bonds might not be relevant once rings have formed.

From these considerations, a hypothetical model that may account for the three-dimensional structures of the two SLO molecules is presented in Fig. 10. According to the model, the basal parts of both molecules are the columnar structures that have the three dimensions of the bottom parts of SLO-I and SLO-O: they are 3.8 nm long, 2.4 to 2.5 nm wide, and 5.0 nm high and 4.5 nm long, 2.4 to 2.5 nm wide, and 5.0 nm high, respectively. The head parts of both molecules have the same basal areas but are 3.2 nm high. Each part of the individual SLO molecules is connected via a narrow polypeptide neck of ca. 1.6 nm in length. There may be a hydrophobic region on the convex side of the basal part of SLO-O for entry into the apolar domain of a lipid bilayer, and there may be a hydrophilic site on the concave side of the basal part of SLO-I for formation of a hole. An —SH group may possibly be located on the hydrophobic site of

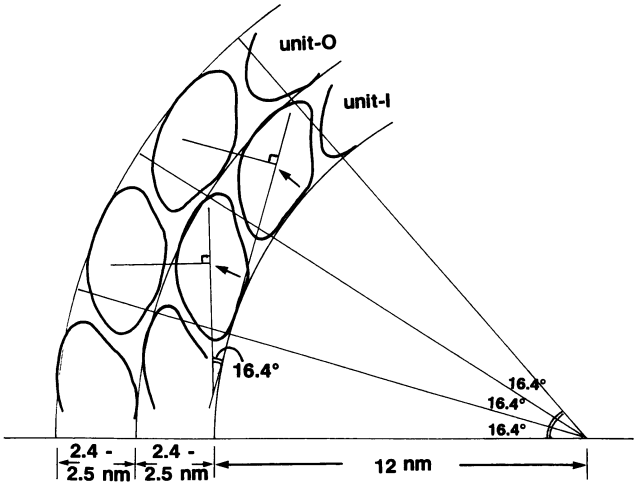

FIG. 7. Schematic drawing of the arrangement of unit-I's and unit-O's. Unit-I's are arrayed with a tilt of 16.4° and overlap each other partially. Unit-O's are arranged parallel to each unit-I, and each makes a pair of a unit-I and a unit-O. The centers of each SLO are arrayed alternately, as viewed from the center of the ring (arrows).

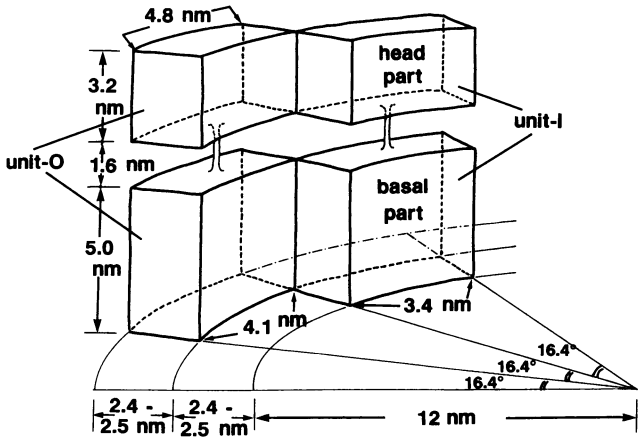

FIG. 9. Schematic drawing of the units. In the case of a ring with an inner diameter of 24 nm and 22 pairs of units, the calculated volume for unit-I is 77 nm^3 and that for unit-O is 88 nm^3.

SLO-O, and cholesterol may interact with bilateral sites on SLO-I to connect each molecule to form a ring.

It is proposed that SLO molecules associate to form rings as shown in Fig. 11. SLO-I molecules connect with one

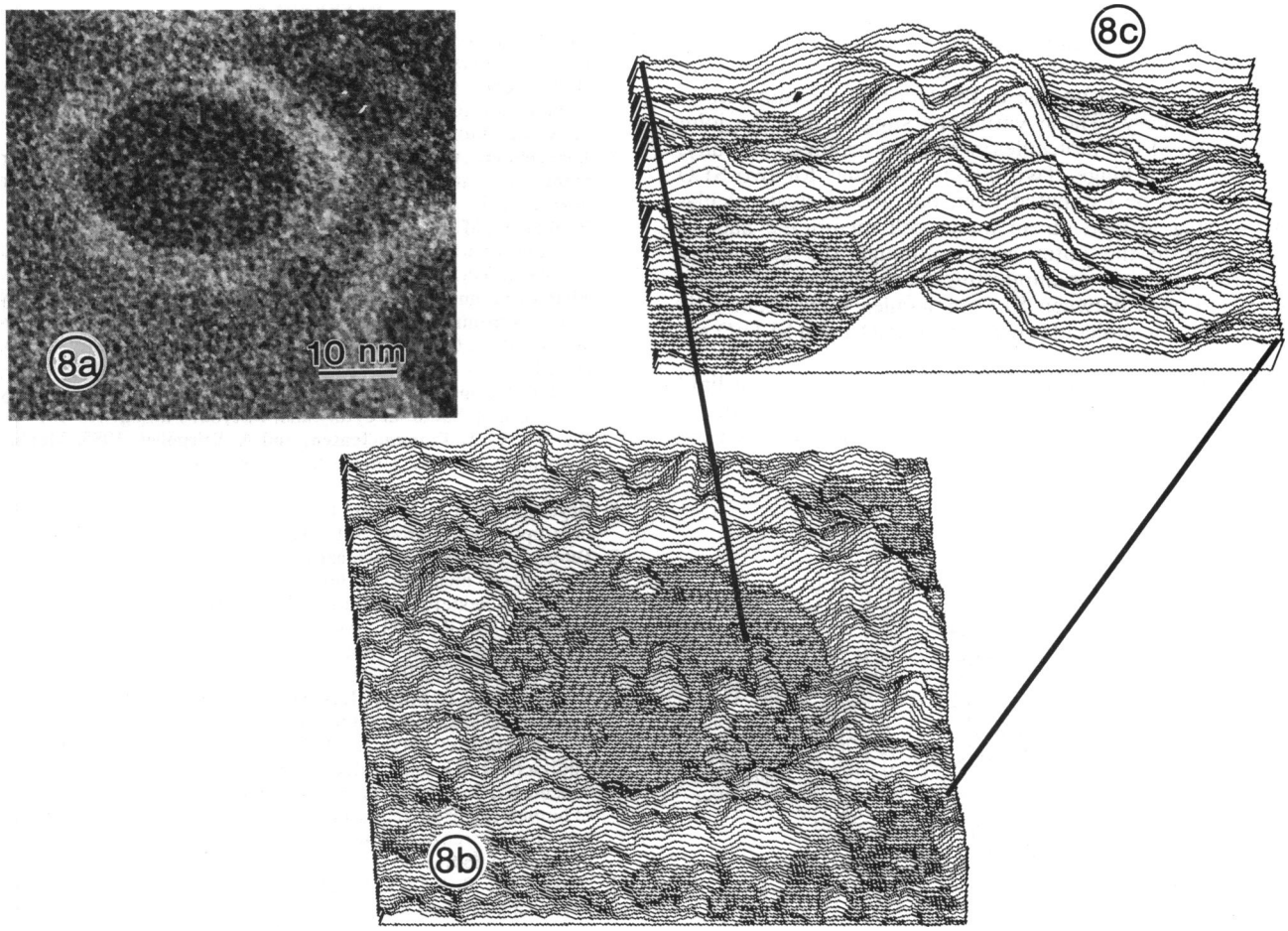

FIG. 8. Electron micrograph of a ring on a ghost membrane (a), which was analyzed three-dimensionally by the image analyzer (b and c). Note that the pair of layers and pairs of units are confirmed but that the arrangement of units has been partially disturbed by noise from ghost membranes.

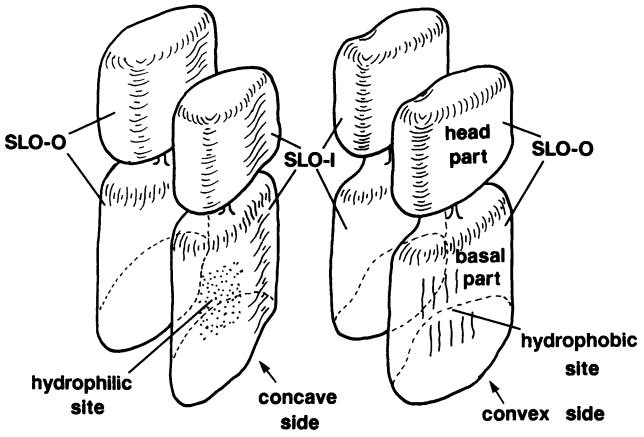

FIG. 10. Schematic drawing of a pair of SLO molecules, SLO-I and SLO-O, anchored in the erythrocyte membrane. Each of the two SLO molecules has a large basal portion connected to a small head portion via a neck of polypeptide. The basal part may have a hydrophobic region with one —SH group, and on the inside, it may have a hydrophilic region. On the sides of basal parts, there may be hinges with receptors for cholesterol.

another with a partial overlap as viewed from the side and are arranged circularly with a minimum of 22 monomers in a complete ring. SLO-O molecules may connect only to SLO-I molecules and not to other SLO-O molecules. The sizes of the rings varied, especially on the ghost membranes (Fig. 3). This variation might be due to the fact that the numbers of visible units vary. These variations suggest that the joint between two SLO-I molecules, which are arranged laterally, is flexible like a hinge. Two distinct volumes for two SLO molecules can be estimated from our geometrical calculations. A ring formed on an intact cell membrane had no visible gaps in the outer layer, although the gear-wheel structures appeared on supporting films without cell membranes and gaps between SLO molecules were seen. It is possible that the molecular weights of SLO-I and SLO-O are the same.

The arcs or rings penetrate an apolar domain of a lipid bilayer with the hydrophobic zone on their convex side. A hole faces a hydrophilic zone on the concave side, and the lipid bilayer is repelled from the hole. The structure of the free edge of the lipid bilayer remains unknown.

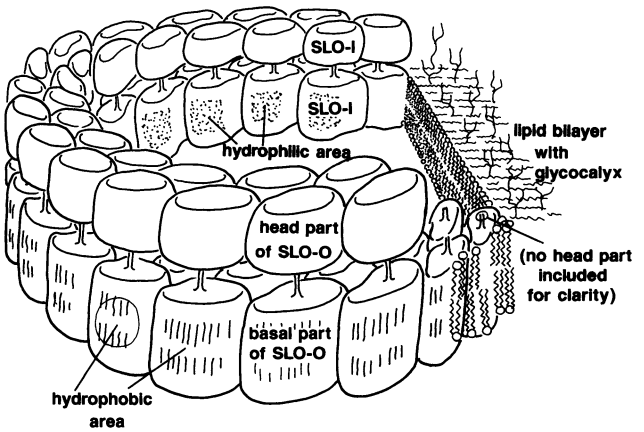

FIG. 11. Schematic drawing of the model of a ring. Rows of SLO-I molecules and SLO-O molecules are shown. See the Discussion for details.

A mechanism for the process of hemolysis induced by SLO is proposed as follows. SLO monomers activated by thiol compounds penetrate the cell membrane individually. SLO-I molecules then encounter each other and form oligomers, and SLO-O molecules connect with SLO-I oligomers. Although, at an early stage, the short arcs may not be associated with a hole, after the arcs have grown into semicircles, the tension of cell membranes on the concave side of arcs is overcome by repulsive forces and holes are formed. The arcs then continue to elongate until rings are complete.

In conclusion, from the new findings obtained by sensitive electron microscopic techniques, a model of SLO molecules and of the ultrastructure of a ring with a crown has been proposed. The role of Cys residues and cholesterol molecules in the interconnections between SLO molecules has been examined, and a new hypothesis has been presented about the mechanism of hemolysis by SLO.

ACKNOWLEDGMENTS

We thank Noboru Nakagawa, The Kitasato Institute, for kindly supplying the SLO and Jun Suzuki and Sadao Kobayashi, Azabu University, and Yasukiyo Nakase, Kitasato University, for their helpful suggestions.

REFERENCES

1. **Alouf, J. E.** 1980. Streptococcal toxins (streptolysin O, streptolysin S and erythrogenic toxin). Pharmacol. Ther. **11**:661–717.
2. **Bernheimer, A. W., L. S. Avigad, and K. S. Kim.** 1979. Comparison of metridiolysin from the sea anemone with thiol-activated cytolysins from bacteria. Toxicon **17**:69–75.
3. **Bernheimer, A. W., and B. Rudy.** 1986. Interactions between membranes and cytolytic peptides. Biochim. Biophys. Acta **864**:123–141.
4. **Bhakdi, S., M. Roth, A. Sziegoleit, and J. Tranum-Jensen.** 1984. Isolation and identification of two hemolytic forms of streptolysin-O. Infect. Immun. **46**:394–400.
5. **Bhakdi, S., and J. Tranam-Jensen.** 1985. Membrane damage by channel-forming proteins: staphylococcal α toxin, streptolysin-O and the C5-9 complement complex. Biochem. Soc. Symp. **50**:221–233.
6. **Bhakdi, S., and J. Tranum-Jensen.** 1986. Membrane damage by pore forming bacterial cytolysins. Microb. Pathog. **1**:5–14.
7. **Bhakdi, S., J. Tranum-Jensen, and A. Sziegoleit.** 1985. Mechanism of membrane damage by streptolysin-O. Infect. Immun. **47**:52–60.
8. **Bryan, J., and L. Wilson.** 1971. Are cytoplasmic microtubules heteropolymers? Proc. Natl. Acad. Sci. USA **8**:1762–1766.
9. **Duncan, J. L., and R. Schlegel.** 1975. Effect of streptolysin O on erythrocyte membranes, liposomes, and lipid dispersions. A protein-cholesterol interaction. J. Cell Biol. **67**:160–173.
10. **Erickson, H. P.** 1974. Assembly of microtubules from preformed, ring-shaped protofilaments and 6-S tubulin. J. Supramol. Struct. **2**:393–411.
11. **Kehoe, M. A., L. Miller, J. A. Walker, and G. J. Boulnois.** 1987. Nucleotide sequence of the streptolysin O (SLO) gene: structural homologies between SLO and other membrane-damaging, thiol-activated toxins. Infect. Immun. **55**:3228–3232.
12. **Mitsui, K., T. Sekiya, Y. Nozawa, and J. Hase.** 1979. Alteration of human erythrocyte plasma membranes by perfringolysin O as revealed by freeze-fracture electron microscopy. Biochim. Biophys. Acta **554**:68–75.
13. **Mitsui, K., T. Sekiya, S. Okamura, Y. Nozawa, and J. Hase.** 1979. Ring formation of perfringolysin O as revealed by negative stain electron microscopy. Biochim. Biophys. Acta **558**:307–313.
14. **Nicolson, G. L., and S. J. Singer.** 1971. Ferritin-conjugated plant agglutinins as specific saccharide strains for electron micros-

copy: application to saccharides bound to cell membrane. Proc. Natl. Acad. Sci. USA **68:**942–945.

15. **Niedermeyer, W.** 1985. Interaction of streptolysin-O biomembranes: kinetic and morphological studies on erythrocyte membranes. Toxicon **23:**425–439.
16. **Pinkney, M., E. Beachey, and M. Kehoe.** 1989. The thiol-activated toxin streptolysin O does not require a thiol group for cytolytic activity. Infect. Immun. **57:**2553–2558.
17. **Smyth, C. J., and J. L. Duncan.** 1978. Thiol-activated (oxygen-labile) cytolysins, p. 129–183. *In* J. Jejaszewicz and T. Wadstrom (ed.), Bacterial toxins and cell membranes. Academic Press, London.
18. **Suzuki, J., S. Kobayashi, K. Kagaya, and Y. Fukazawa.** 1988. Heterogeneity of hemolytic efficiency and isoelectric point of streptolysin O. Infect. Immun. **56:**2474–2478.
19. **Tranam-Jensen, J., S. Bharkdi, B. Bhakdi-Lehnen, O. J. Bjerrum, and V. Speth.** 1978. Complement lysis: the ultrastructure and orientation of the C5-9 complex on target sheep erythrocyte membranes. Scand. J. Immunol. **7:**45–56.
20. **Tweten, R. K.** 1988. Nucleotide sequence of the gene for perfringolysin O (theta-toxin) from *Clostridium perfringens*: significant homology with the genes for streptolysin O and pneumolysin. Infect. Immun. **56:**3235–3240.
21. **Wannamaker, L. W.** 1983. Streptococcal toxins. Rev. Infect. Dis. **5:**S723–S732.